

Quantum Dots Luminescence Collection Enhancement and Nanoscopy by Dielectric Microspheres

Francesco Biccari,* Travis Hamilton, Andrea Ristori, Stefano Sanguinetti, Sergio Bietti, Massimo Gurioli,* and Hooman Mohseni

In recent years, dielectric microspheres have been used in conjunction with optical microscopes to beat the diffraction limit and to obtain superresolution imaging. The use of microspheres on quantum dots (QDs) is investigated, for the first time, to enhance the light coupling efficiency. The enhancement of the QD luminescence collection in terms of extraction and directionality is demonstrated, as well as the enhancement of spatial resolution. In particular, it is found that a dielectric microsphere, placed on top of an epitaxial QD, increases the collected radiant energy by about a factor of 42, when a low numerical aperture objective is used. Moreover, if two or more QDs are present below the microsphere, the modification of the far field emission pattern allows selective collection of the luminescence from a single QD by simply changing the collection angle. Dielectric microspheres present a simple and efficient tool to improve the QD spectroscopy, and potentially QD-based devices.

Nano-optics is a well-established topic dealing with the study of the interaction between materials and light at the nanoscale; it addresses a very wide spectrum of goals ranging from quantum electrodynamics to sensors.^[1] One important branch of nano-optics is the nanospectroscopy, which aims to combine the subwavelength spatial resolution with a large variety of spectroscopic techniques.^[2,3] Historically, it has been pioneered by the invention of Scanning Near-field Optical

Microscopy (SNOM) in the 1980s.^[1,2] Many different approaches demonstrated the powerfulness of SNOM in detecting the details of the near field around an emitter in a nanoresonator. SNOM still remains a niche spectroscopic tool, owing to both costs and difficulties in using it, in particular in a cryogenic setup needed for spectrally pure quantum emitters, such as semiconductor quantum dots (QDs). A simpler but less performing approach for QDs, developed in the 1990s, is based on solid immersion lenses (SILs).^[4] Other techniques, developed in the 2000, like STED, BLINK and PALM/STORM, are very powerful but their use is limited only to specific fluorophores used for the staining of the sample and therefore they are not suitable for spectroscopic analysis of generic nanoemitters.^[5]

A significant issue in nanospectroscopy is the large mismatch between the light wavelength and the nanomaterials size, which usually leads to a weak interaction and subsequently a small efficiency of coupling to the emitted or scattered light at the nanoscale.^[6] Indeed, a sister problem of the spatial resolution improvement is the enhancement of the collected light, which is related also to the practical problem to increase the directionality of the luminescence from nanoemitters toward external components (e.g., optical fibers). In order to focus on a specific example, let us consider the luminescence collection from epitaxial QDs.^[7] The QD size is in the range of 10 nm, they are buried in a dielectric with large refractive index and they need to operate at cryogenic temperatures, limiting the numerical aperture (NA) of the collecting objective. Given these constraints, coupling the QD emission into a controlled optical channel is a relevant challenge in quantum communication. Excellent extraction efficiency has been obtained by photonic cavities, where, however, the spatial and spectral matching between the QD and the cavity must be better than 50 nm and 1 meV, respectively.^[5] In order to tackle this problem, several broadband photonic devices have been proposed:^[8–18] a state of the art approach is represented by photonic trumpets (PTs).^[17] However, these approaches suffer from the problem of spatial matching between the photonic modes and the QDs, since the QD needs to be at the center of the photonic modes for an optimal coupling. This requirement asks for complex nanofabrication and/or nanomanipulation and strongly limits the scalability of these solutions, not to mention that these approaches (cavities and trumpets) are irreversible, expensive, and subject


Dr. F. Biccari, A. Ristori, Prof. M. Gurioli
Department of Physics and Astronomy
University of Florence
Via G. Sansone 1, I-50019 Sesto Fiorentino (FI), Italy
E-mail: francesco.biccari@unifi.it; massimo.gurioli@unifi.it

Dr. F. Biccari, A. Ristori
LENS - European Laboratory for Non-Linear Spectroscopy
University of Florence
Via N. Carrara 1, I-50019 Sesto Fiorentino (FI), Italy

T. Hamilton, Prof. H. Mohseni
Bio-Inspired Sensors and Optoelectronics Laboratory
Northwestern University
2145 Sheridan Rd, Evanston, IL 60208, USA

Prof. S. Sanguinetti, Dr. S. Bietti
Department of Material Science
University of Milano-Bicocca
Via Cozzi 55, I-20125 Milano, Italy

Prof. M. Gurioli
Instituto de Ciencia de los Materiales
Universidad de Valencia
P.O. Box 22085, 46071 Valencia, Spain

 The ORCID identification number(s) for the author(s) of this article can be found under <https://doi.org/10.1002/ppsc.201900431>.

DOI: 10.1002/ppsc.201900431

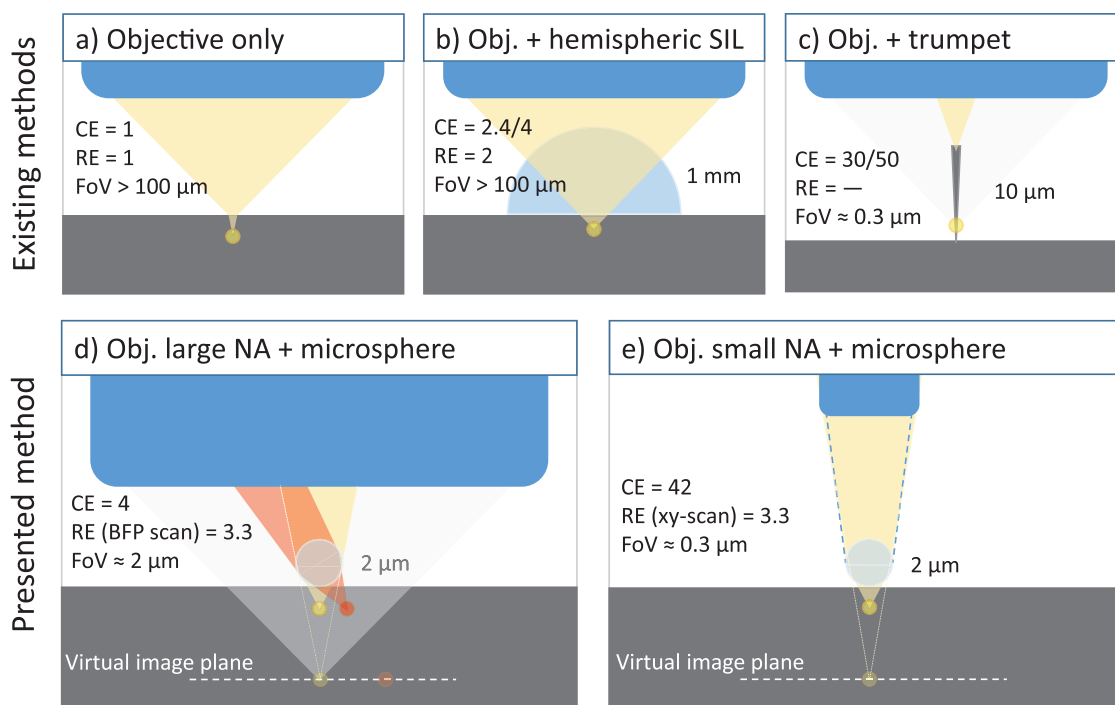


Figure 1. Comparison of the collection enhancement (CE), resolution enhancement (RE) and field of view (FoV) between several experimental microscopy systems in the case of a dipole buried in a material with a refractive index $n = 3.5$. The gray area represents the maximal acceptance angle of the objective. The pale yellow or and the pale red areas represent the emission of the dipole collected by the objective. The yellow and red circles represent the position of the dipoles. The draw is not in scale. When two numbers are given, they refer to NA = 0.1 and NA = 0.7, respectively. a) Single objective (reference); b) objective and hemispherical SIL with $n = 2$; c) objective with photonic trumpet; d,e) objective and microsphere for NA = 0.7 and NA = 0.1, respectively. In panels d and e, the virtual image planes are also reported.

to possible failure in the nanofabrication process. Alternatively, an old, but still valid approach, both spectrally and spatially tolerant, is the SIL.^[4,19] SIL is a broadband tool giving an increase of spatial resolution and light extraction, which can be easily and reversibly placed on the sample and it does not require any special processing. However, SIL can enhance the light collection only by a factor equal to its refractive index n , since the NA of the system is increased by a factor n , at most. Moreover, the far field profile is not optimal, especially for small NA objective or for collecting light in an optical fiber.

In the last decade, dielectric microspheres attracted a lot of attention from the scientific community. Their peculiarity consists in the formation, when illuminated, of a photonic jet on the shadow side of the structure with a beam size down to one third the wavelength of incident light.^[20] The photonic properties of a microsphere are illustrated in the Supporting Information. They were used in optical data extraction,^[21] Raman spectroscopy measurements,^[22,23] enhancement of luminescence collection,^[24–26] superresolution microscopy,^[27–29] and many other fields. Still the use of microspheres for quantum emitters nanospectroscopy has not yet demonstrated or tested, despite the raising interest in quantum communication and information emerged in the last few years.

In this paper we use, for the first time, dielectric microspheres to achieve a high coupling enhancement between quantum emitters with high spatial (500 nm) and spectral (100 meV) tolerance. In order to test our approach, we focus on QDs nanospectroscopy, showing the advantage of our approach

on luminescence collection, spatial resolution and directionality, with respect to other broadband solutions, like SILs (low enhancement) and PTs (low spatial tolerance). In this way, we essentially combine the advantage of a simple, cost-effective, broadband postgrowth approach with the photonic tailoring of the light modes, leading to a large enhancement of the photoluminescence (PL) and to the ability to distinguish QDs below the diffraction limit.

In order to clarify the novelty of our approach, in **Figure 1** we have compared the effect of a microsphere (Figure 1d,e) with respect to a single objective^[30] (Figure 1a), a hemispherical SIL^[4,19] (Figure 1b) and a photonic trumpet^[17,31] (Figure 1c). The quantities of interest are: 1) collection enhancement (CE) defined as the ratio between the power collected by the objective with the sphere over the power collected by the same objective without the sphere; 2) resolution enhancement (RE) defined as the ratio between the resolution of the system with the sphere over the resolution of the same system without the sphere; 3) field of view (FoV). We have reported these three quantities for all the optical systems listed above in the case of a dipole immersed in a material with a refractive index $n = 3.5$, emitting at 720 nm. In the case of the microsphere, in order to perform single quantum dot spectroscopy, two different approaches are given, one for large NA (Figure 1d) and one for small NA (Figure 1e). Indeed, as we will see in this paper, for large NA it is preferable to keep the microsphere fixed on the sample and select the luminescence of the QD by spatially filtering the image with a pin-hole in the image plane or, better,

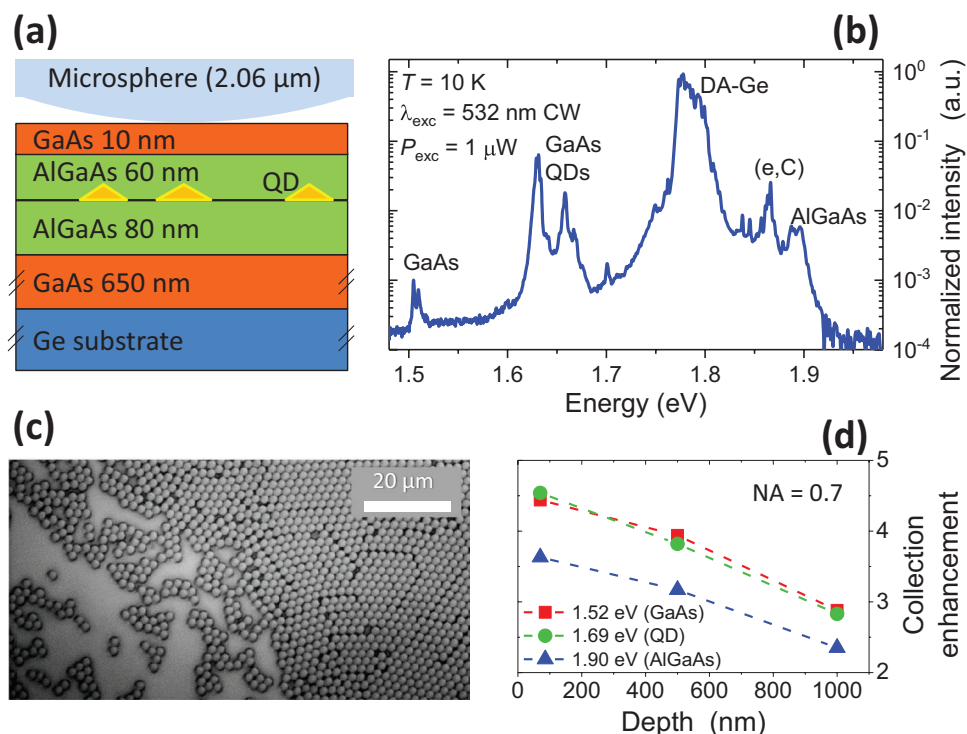


Figure 2. a) Scheme of the section of the sample and a microsphere on top of it. b) Typical PL spectrum of the sample. c) Microscope image of the sample surface after microsphere deposition. The picture shows an area where both a compact array and isolated microspheres are present. d) Theoretical collection enhancement for NA = 0.7 and $\lambda = 720$ nm, at different depths of the buried emitters, with respect to a single objective of the same NA.

in the back focal plane (BFP) of the objective; whereas for small NA this pin-hole selection is useless, since the FoV is similar to the resolution or, analogously, the BFP is completely illuminated: it is more useful to attach the microsphere directly to the collecting optics (objective, optical fiber, ...) and spatially scan the sample (see Figure S1f of the Supporting Information).

In order to analyze the effect of microspheres on the PL emitted by single photon emitters, we performed an experimental study of a sample containing a layer of QDs buried 70 nm below the surface and emitting in the range 1.60–1.72 eV (see Figure 2a,b). Silicon dioxide microspheres with diameter of 2.06 μm were deposited onto the sample surface using a self-assembly convection method (see Figure 2c). Details about sample growth and spheres deposition are reported in the experimental section. The size of the microspheres has been chosen because it gives a large collection enhancement for a wide range of wavelengths, from visible to near infrared (see Supporting Information). In Figure 2d, we report the simulated collection enhancements for a NA = 0.7 objective at three different wavelengths, as a function of the depth of the buried emitter (details can be found in the Supporting Information).

In order to analyze the improvement in the PL collection, we compared several QD emissions without the presence of the spheres with emissions of QDs found under spheres. In Figure 3a,b we have reported two microscope images of two different parts of the sample: one where the spheres are almost absent, and the other one with a packed array of spheres. We acquired hyperspectral PL maps over these areas. The PL intensity maps of the QD emission, obtained by the integration

of the hyperspectral maps between 1.60 and 1.72 eV, are superimposed to the corresponding optical images in a blue-red color code. The spots in Figure 3b refer to QDs below the sphere and their emission is much more intense with respect to the emission from QDs of Figure 3a. Note that in Figure 3a we can count roughly 1 QD per 20 μm² and QDs with high emissions are even sparser. This helps in resolving single QDs (at most one per microsphere), but complicates the analysis of the microsphere enhancement of QD PL. Indeed, there is a low chance for a good QD to be located exactly below the center of a silica sphere.

The total PL intensity enhancement (E_{tot}) is given by the product of the excitation enhancement (E_x) and collection enhancement (CE). In order to find separately these two factors, we used the saturation effect of the QD emission (see Supporting Information for more details). Indeed, the PL intensity, I_{PL} , of a QD as function of the excitation power P has a saturation point, which can be used as reference in order to compare excitation powers in different excitation conditions. The maximum corresponds to the condition of having on average one exciton in the QDs. Therefore we can compare the excitation power at saturation P_{sat} with and without spheres as an estimate of the increased power density due to the photonic nanojets: $E_x = P_{\text{sat}}^s / P_{\text{sat}}^o$, where the apex “s” and “o” refers to the values with and without a sphere, respectively).

Similarly, we can compare the PL intensity at saturation I_{sat} with and without spheres as an estimate of the increased light extraction due to the photonic nanojets: $\text{CE} = I_{\text{sat}}^s / I_{\text{sat}}^o$. This is possible because at the saturation point the excitation

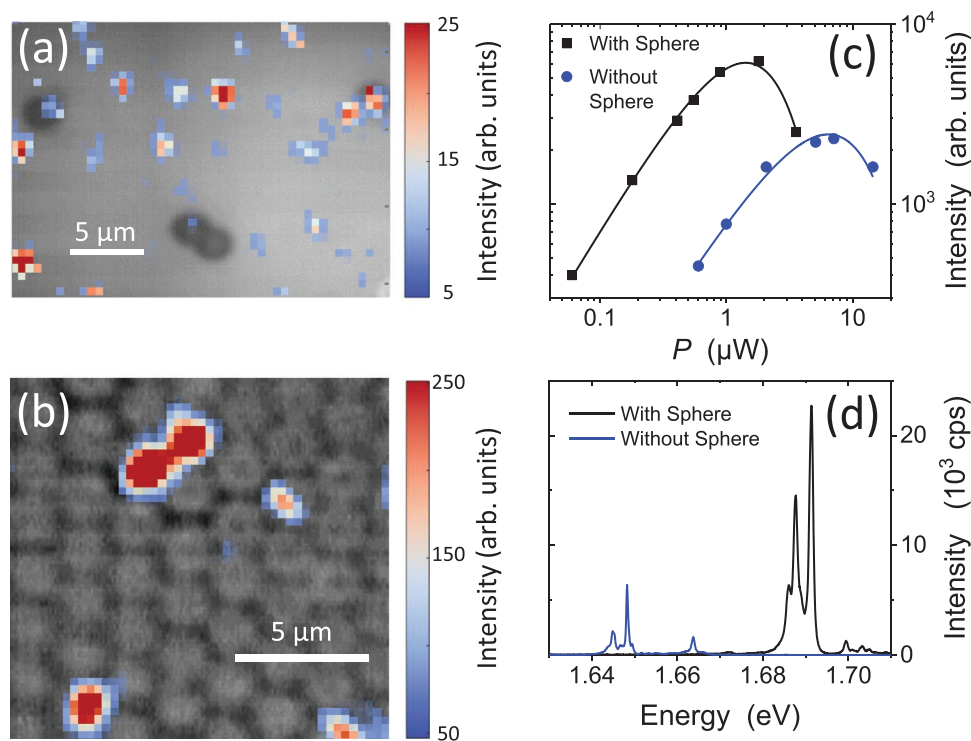


Figure 3. a) Microscope image of an area of the sample where microspheres are very sparse. b) Microscope image of an area of the sample where ordered array of microsphere is present; both in (a) and (b) the PL intensity map of the QD emission, integrated between 1.60 and 1.72 eV, is superimposed to the optical map in a blue-red color code. Pixel dimensions $0.5 \times 0.5 \mu\text{m}^2$ in 1a and $0.25 \times 0.25 \mu\text{m}^2$ in 1b. c) Spectrally integrated PL intensity as a function of the excitation power of two typical QDs without and with microsphere; the saturation condition described in the main text is clearly shown; the continuous lines are fits performed by Equation S1 of the Supporting Information. d) Comparison of the spectra from the brightest QD emissions with and without the spheres.

conditions are identical. It is worth stressing that the two parameters P_{sat} and I_{sat} depend on different mechanisms. For a given QD, since the absorption above bandgap is homogeneous in our sample, P_{sat} measures the QD capture cross section and therefore the efficiency in the carrier relaxation into the QD states. On the contrary, I_{sat} measures the QD radiative efficiency, that is the presence of nonradiative channels competing with spontaneous emission.

By performing a statistical evaluation on 20 different QDs on a part of the sample free from spheres, we get $P_{\text{sat}}^{\text{o}} = (10.0 \pm 3.5)$ mW and $I_{\text{sat}}^{\text{o}} = (6000 \pm 2000)$ cps, where the reported ranges refer to the interval between minimum–maximum values. Typical values of saturation curves with and without the spheres are given in Figure 3c. However, since the alignment of the sphere with the QD position (which has a very relevant role as shown in Figure S1 of the Supporting Information) is random, in order to properly estimate the optimal photonic jet enhancement, the data without spheres must be compared only with the best values obtained by QD emission under the sphere, which are $P_{\text{sat}}^{\text{s}} = 1.2$ mW and $I_{\text{sat}}^{\text{s}} = 22\,000$ cps. The spectra from the brightest QD emissions with and without the spheres are reported in Figure 3d. With this assumption, the photonic nanojets enhancement is very clear, giving a factor $E_x = 8 \pm 2$ and a factor of CE = 4 ± 1 . These values are in very good agreement with the simulated data: the expected excitation enhancement, averaged below the sphere, is about 9 (simulations not

shown) while the expected collection enhancement is about 4.5 (see Figure S1 of the Supporting Information).

Three are the mechanisms behind the collection enhancement (in order of importance): enhancement of the emitted power extracted from the sample surface, modification of the power emission pattern due to the lensing effect of the microsphere, which increases the power emitted toward the direction normal to the surface, and enhancement of the emitted power from the source by Purcell effect. The enhancement of the emitted power from the sample surface is due to the reduction of the total internal reflection at the air/sample interface. This is caused by the evanescent wave coupling between the sample and the microsphere. Quantification of these effects were performed by FDTD simulations reported in Figure S2 (Supporting Information). In particular, the concentration of the far-field emission pattern toward the normal direction makes the microspheres a NA increasing tool, making a low NA objective similar to a large NA objective.

Finally, we want to address the link between spatial resolution and NAs of the objective collecting light from the QDs. This has been realized by introducing a pinhole in the collimated region of the PL signal after the objective with NA = 0.7; the estimated NA with the selected pinhole was NA = 0.05. By scanning the pinhole position in the plane perpendicular to the light propagation, we have realized an angular (momentum k) filter for the collected emission. We selected a sphere where

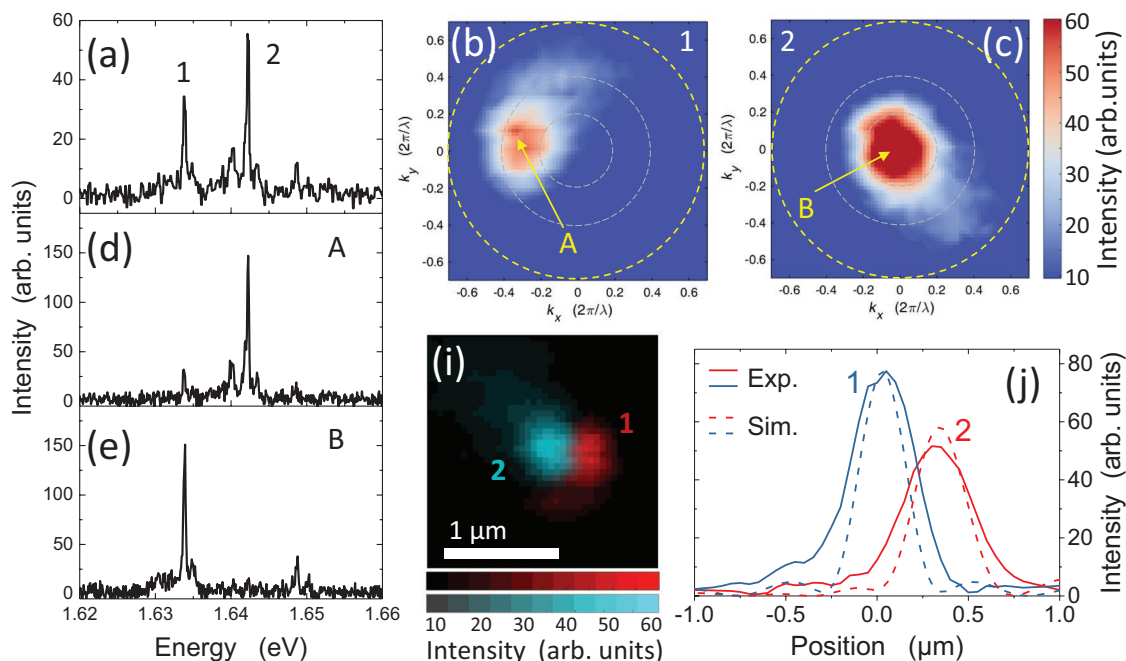


Figure 4. a) QD-PL spectrum collected with a microsphere and objective with NA = 0.7; we highlighted the emission of two QDs, labeled with 1 and 2. b,c) k -space maps of the QD-PL emission integrated over the emission energy of QD 1 and 2, respectively. In the maps, the three yellow circles represent NA = 0.2, NA = 0.4, and NA = 0.7. d,e) PL spectra of the point A (in panel b) and point B (in panel c), respectively, obtained by filtering the emission in k -space by a pin-hole with an aperture corresponding to NA = 0.05. i) Real space map of the emission of the two QDs obtained by a proper transformation of the k -space maps of panel b and c (see Equation S2 of the Supporting Information). j) Cuts of the map in panel i along the direction joining the two centers (continuous lines). The dashed lines represent the same cuts applied on the simulated spatial map (see Figure S5 of the Supporting Information).

two different QD emissions were observed; the spectrum for each is provided in Figure 4a. The k -space PL image is obtained by scanning the pinhole and the resulting maps for QD1 and QD2 are presented in Figure 4b,c, respectively. In both maps, the yellow circle with the highest diameter refers to the NA = 0.7 of our objective. As expected, we observe that the sphere on the sample has a focusing effect. Indeed, the NA of the emission from the microsphere is estimated to be about 0.2, which is much smaller than the NA of our objective lens.

In addition, we see that the QDs in the k -space maps are displaced. This is highlighted in the PL spectra presented in Figure 4d,e by collecting light from different locations of the k -space associated with the two QDs (points A and B of Figure 4b,c, respectively). The real space maps, obtained by applying the Equation S2 of the Supporting Information to the experimental data of Figure 4b,c, are reported and superimposed in Figure 4i, where it is evident that the displacement in k -space maps is due to a spatial displacement of the QDs in real space. The displacement is about 300 nm. It is worth noting that the same image, without spectral information, could be obtained by a direct imaging of the virtual focal plane, as in the regular use of microspheres for super-resolution microscopy. However, our approach allows to obtain a hyperspectral map (a spectrum for each spatial point) simply scanning in k -space, much easier than a complete image reconstruction and spatial filtering. Moreover, it is also worth noting that this is useful to select the emissions of two or more QDs below a microsphere simply choosing a proper collection angle (for example positioning several optical fibers above the microsphere at different

collection angles) and not after an entire image reconstruction (objective—tubelens—spatial selection).

In Figure 4j, a cross-section of the map in 4i, passing along the centers of the two QDs, is presented, along with the same cross-section for the simulated configuration (see Figure S5 in the Supporting Information). This example shows how powerful is the proposed method in producing a 3D map of emission intensity I_{PL} versus the energy and transverse momentum of the emitted photons.

In summary, we have exploited the unique properties of dielectric microspheres for improved nanospectroscopy of quantum dots in semiconductors. Clear enhancement in excitation power density (a factor 9), light collection (a factor 4), and spatial resolution have been demonstrated using a NA = 0.7 objective, all in good agreement with theoretical predictions. Scaled to a low NA objective (NA = 0.13), this means a collection enhancement about by a factor 42. Our results open the route to exploit dielectric microspheres in many aspects of optical nanospectroscopy. In a single-mode realization, we envision highly efficient scanning near field optical microscopy by fabricating a near field tip that is made of a microsphere attached to a single-mode optical fiber. A similar approach, using a scanning microsphere and a microscope was already implemented for optical nanoscopy.^[32] For a multimode realization, we envision highly efficient extraction of entangled photon pairs at different wavelengths from different QDs using the broadband nature and spatial resolution of our approach. Moreover, studying the angular emission pattern of a microsphere position on top of two QDs 300 nm apart, we have shown that

it is possible to monitor two different QDs placed in the field of view of the microsphere, simply collecting light at different angles, for example, for photon indistinguishability measurements. In our current experiment, a possible drawback is the deterministic positioning of the microspheres to the points of interest. However, we believe that modern nanomanipulation techniques could provide accurate positioning of microspheres leading to efficient extraction of well-collimated far-field beams of the flying entangled qubits from arrays of quantum emitters. In addition, the exploitation of photonic nanojet in combination with particular laser-writable materials, like GaAsN:H,^[33] could allow to fabricate QDs directly under the microspheres.

Experimental Section

Sample Preparation: All the experiments were performed on a single sample containing GaAs QDs in a matrix of Al_{0.3}Ga_{0.7}As. The sample was grown in a conventional GEN II solid-source molecular beam epitaxy (MBE) system on a Ge substrate. The structure is the following: a GaAs buffer layer (650 nm) deposited on a Ge (001) substrate miscut 6° toward [110] direction; an Al_{0.3}Ga_{0.7}As barrier layer (80 nm); a layer of GaAs QD formed by Droplet Epitaxy (average height 10 nm) surrounded by a barrier of Al_{0.3}Ga_{0.7}As (60 nm); a GaAs capping layer (10 nm) was finally grown on top. The samples were processed with postgrowth rapid thermal annealing RTA process for 4 min at 700 °C in nitrogen atmosphere. Growth details are reported elsewhere.^[34] The sketch of the sample is given in Figure 2a and a typical PL spectrum is reported in Figure 2b. The spectrum shows different contributions. The different bands are attributed to: excitonic recombinations in the 650 nm thick GaAs buffer layer (1.506 and 1.511 eV), QD emission (1.60–1.72 eV), recombination from donor–acceptor (DA) pair due to the germanium impurities diffused in the AlGaAs layer (1.75–1.82 eV), electron to acceptor carbon level impurity in AlGaAs layer (1.855–1.870 eV), and finally bound exciton recombinations in the AlGaAs layer (1.890 and 1.900 eV). These attributions are labeled in the spectrum; note also that the QD emission stems from many QDs and the individual lines are not resolved here.

Microsphere Deposition: Silicon dioxide microspheres with diameters of 2.06 μm and a standard deviation of 0.05 μm were used (Microparticles GmbH). The microspheres come in aqueous suspension making up 5% of the weight/volume percentage. The microspheres were deposited onto the GaAs QD sample using a self-assembly convection method.^[35] An aqueous suspension of microspheres was deposited between the sample and a glass slide. The microsphere solution naturally forms a meniscus between the glass slide and sample where a monolayer of hexagonally close packed microspheres forms. By dragging the glass slide across the sample, the spheres exit the meniscus while keeping their hexagonally close packed distribution.^[36] The microspheres exit the meniscus easier when the sample is treated by and oxygen plasma cleaner. The cleaner causes the surface of the sample to change from hydrophobic to hydrophilic. Moreover, a perfectly cleaned surface ensures that no air gap exists between the spheres and the sample surface. However, a small gap of few tens of nm is not detrimental for the jet formation (see Figure S3 of the Supporting Information). By increasing the speed of deposition, the authors were able to deposit a loose packed array of microspheres on the sample surface. The loosely packed microsphere regions are characterized by QDs with and without microspheres in close proximity to one another in order to make quick and efficient PL measurements. In Figure 2c, an optical microscopy image of the sample covered by the spheres is reported. It is worth noting the different emissions in our sample arise from different layers and then from different depths, which is quite relevant in our discussion. In particular, the GaAs QDs are buried 70 nm below the surface, the AlGaAs emission is confined in a region between 10 and 150 nm from the surface, and the GaAs emission is from a region between

150 and 800 nm from the surface. In Figure 2d, we report the simulated collection enhancements at three different wavelengths, corresponding to the QDs, AlGaAs, and GaAs emissions, as a function of the depth of the buried emitter. The simulation is based on the model discussed in the Supporting Information. These data show that minor differences are expected between AlGaAs and the QDs, while a lower collection enhancement is predicted for the GaAs emission.

Photoluminescence Measurements: The optical properties of the fabricated nanostructures were studied by microphotoluminescence (micro-PL). The sample was kept at 10 K in a low-vibration continuous He-flow cryostat (Janis ST-500), which in turn was mounted on a x–y translation stage (Physik Instrumente) for scanning the sample surface. The luminescence was collected by a home-made confocal microscope setup equipped with an infinity corrected 100× objective (Mitutoyo 378-806-3, NA = 0.7). The luminescence was spectrally dispersed and detected using a spectrograph (an Acton SP2300i) with a 600 g mm⁻¹ grating and a 1200 g mm⁻¹ grating, blazed at 1000 nm and 750 nm respectively, and a Si CCD (Acton Pixis 100F). The spatial resolution of the system is about 500 nm, while the spectral resolution is about 400 μeV using the 600 g mm⁻¹ grating and 250 μeV using the 1200 g mm⁻¹ grating. For time-integrated measurements, the excitation source was a CW diode-pumped solid-state laser at 532 nm (CNI MLL-III-532).

Supporting Information

Supporting Information is available from the Wiley Online Library or from the author.

Acknowledgements

Research at the University of Florence was supported by the Italian Ministry for Education, University and Research within the Futuro in Ricerca (FIRB) program (project DeLIGHTeD, Protocollo RBF12RS1W) and by Fondazione Cassa di Risparmio di Firenze within the project PERBACCO 2016.1084. Research at Northwestern University was partially supported by ARO award # W911NF-11-1-0390.

Conflict of Interest

The authors declare no conflict of interest.

Keywords

microspheres, near field, photoluminescence, photonic nanojet

Received: October 29, 2019
Published online: December 15, 2019

- [1] L. Novotny, B. Hecht. *Principles of Nano-Optics*, Cambridge University Press, Cambridge **2012**.
- [2] A. Zayats, D. Richards. *Nano-Optics and Near-Field Optical Microscopy*, Artech House, Norwood, MA/London **2008**.
- [3] C. Cremer, B. R. Masters, *Eur. Phys. J. H* **2013**, *38*, 281.
- [4] K. A. Serrels, E. Ramsay, P. A. Dalgarno, B. D. Gerardot, J. A. O'Connor, R. H. Hadfield, R. J. Warburton, D. T. Reidet, *J. Nanophotonics* **2008**, *2*, 021854.
- [5] S. J. Sahl, S. W. Hell, S. Jakobs, *Nat. Rev. Mol. Cell Biol.* **2017**, *18*, 685.
- [6] P. J. Schuck, D. P. Fromm, A. Sundaramurthy, G. S. Kino, W. E. Moerner, *Phys. Rev. Lett.* **2005**, *94*, 017402.

- [7] *Single Semiconductor Quantum Dots* (Ed: P. Michler), Springer, Berlin, Heidelberg, **2009**.
- [8] E. Viasnoff-Schwoob, C. Weisbuch, H. Benisty, S. Olivier, S. Varoutsis, I. Robert-Philip, R. Houdré, C. J. M. Smith, *Phys. Rev. Lett.* **2005**, *95*, 183901.
- [9] T. Lund-Hansen, S. Stobbe, B. Julsgaard, H. Thyrrstrup, T. Süner, M. Kamp, A. Forchel, P. Lodahl, *Phys. Rev. Lett.* **2008**, *101*, 113903.
- [10] Q. Quan, I. Bulu, M. Lončar, *Phys. Rev. A* **2009**, *80*, 011810.
- [11] A. Akimov, A. Mukherjee, C. L. Yu, D. E. Chang, A. S. Zibrov, P. R. Hemmer, H. Park, M. D. Lukin, *Nature* **2007**, *450*, 402.
- [12] J. Claudon, J. Bleuse, N. S. Malik, M. Bazin, P. Jaffrennou, N. Gregersen, C. Sauvan, P. Lalanne, J.-M. Gérard, *Nat. Photonics* **2010**, *4*, 174.
- [13] T. M. Babinec, B. M. Hausmann, M. Khan, Y. Zhang, J. R. Maze, P. R. Hemmer, M. Lončar, *Nat. Nanotechnol.* **2010**, *5*, 195.
- [14] J. Heinrich, A. Huggenberger, T. Heindel, S. Reitzenstein, S. Höfling, L. Worschech, A. Forchel, *Appl. Phys. Lett.* **2010**, *96*, 211117.
- [15] M. Gschrey, A. Thoma, P. Schnauber, M. Seifried, R. Schmidt, B. Wohlfeil, L. Krüger, J.-H. Schulze, T. Heindel, S. Burger, F. Schmidt, A. Strittmatter, S. Rodt, S. Reitzenstein, *Nat. Commun.* **2015**, *6*, 7662.
- [16] M. E. Reimer, G. Bulgarini, N. Akopian, M. Hocevar, M. B. Bavinck, M. A. Verheijen, E. P. Bakkers, L. P. Kouwenhoven, V. Zwiller, *Nat. Commun.* **2012**, *3*, 737.
- [17] M. Munsch, N. S. Malik, E. Dupuy, A. Delga, J. Bleuse, J.-M. Gérard, J. Claudon, N. Gregersen, J. Mørk, *Phys. Rev. Lett.* **2013**, *110*, 177402.
- [18] M. Munsch, A. V. Kuhlmann, D. Cadeddu, J.-M. Gérard, J. Claudon, M. Poggio, R. J. Warburton, *Nat. Commun.* **2017**, *8*, 76.
- [19] V. Zwiller, G. Björk, *J. Appl. Phys.* **2002**, *92*, 660.
- [20] H. Yang, R. Trouillon, G. Huszka, M. A. M. Gijs, *Nano Lett.* **2016**, *16*, 4862.
- [21] S.-C. Kong, A. V. Sahakian, A. Heifetz, A. Taflove, V. Backman, *Appl. Phys. Lett.* **2008**, *92*, 211102.
- [22] C. Xing, Y. Yan, C. Feng, J. Xu, P. Dong, W. Guan, Y. Zeng, Y. Zhao, Y. Jiang, *ACS Appl. Mater. Interfaces* **2017**, *9*, 32896.
- [23] I. Alessandri, N. Bontempi, L. E. Depero, *RSC Adv.* **2014**, *4*, 38152.
- [24] D. Gérard, A. Devilez, H. Aouani, B. Stout, N. Bonod, J. Wenger, E. Popov, H. Rigneault, *J. Opt. Soc. Am. B* **2009**, *26*, 1473.
- [25] J. J. Schwartz, S. Stavrakis, S. R. Quake, *Nat. Nanotechnol.* **2010**, *5*, 127.
- [26] Y. Yan, Y. Zeng, Y. Wu, Y. Zhao, L. Ji, Y. Jiang, L. Li, *Opt. Express* **2014**, *22*, 23552.
- [27] Z. Wang, W. Guo, L. Li, B. Luk'yanchuk, A. Khan, Z. Liu, Z. Chen, M. Hong, *Nat. Commun.* **2011**, *2*, 218.
- [28] A. V. Maslov, V. N. Astratov, *Phys. Rev. Appl.* **2019**, *11*, 064004.
- [29] D. Migliozi, M. A. M. Gijs, G. Huszka, *Sci. Rep.* **2018**, *8*, 15211.
- [30] *Handbook of Nanophysics: Nanoparticles and Quantum Dots* (Ed: K. D. Sattler), CRC Press, Boca Raton, FL **2010**.
- [31] P. Stepanov, A. Delga, N. Gregersen, E. Peinke, M. Munsch, J. Teissier, J. Mørk, M. Richard, J. Bleuse, J.-M. Gérard, J. Claudon, *Appl. Phys. Lett.* **2015**, *107*, 141106.
- [32] F. Wang, L. Liu, H. Yu, Y. Wen, P. Yu, Z. Liu, Y. Wang, W. J. Li, *Nat. Commun.* **2016**, *7*, 13748.
- [33] F. Biccari, A. Boschetti, G. Pettinari, F. La China, M. Gurioli, F. Intonti, A. Vinattieri, M. S. Sharma, M. Capizzi, A. Gerardino, L. Businaro, M. Hopkinson, A. Polimeni, M. Felici, *Adv. Mater.* **2018**, *30*, 1705450.
- [34] L. Cavigli, M. Abbarchi, S. Bietti, C. Somaschini, S. Sanguinetti, N. Koguchi, A. Vinattieri, M. Gurioli, *Appl. Phys. Lett.* **2011**, *98*, 103104.
- [35] B. G. Prevo, O. D. Velev, *Langmuir* **2004**, *20*, 2099.
- [36] W. Wu, Q. He, C. Jiang, *Nanoscale Res. Lett.* **2008**, *3*, 397.